

Ion-Specific Effects on the Structure, Size, and Charge of Polymers Applied in Enhanced Oil Recovery

Zsófia Vargáné Árok, Szilárd Sáringer, Gréta Papp, Ádám Juhász, Sándor Puskás, and Istvan Szilagyí*




Cite This: *Energy Fuels* 2024, 38, 6798–6805



Read Online

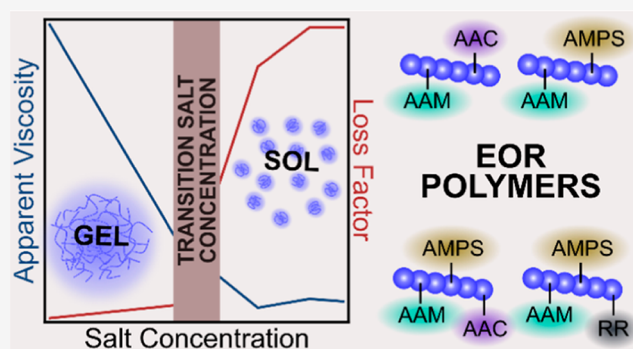
ACCESS |

 Metrics & More

 Article Recommendations

 Supporting Information

ABSTRACT: Polymers are widely applied in enhanced oil recovery (EOR) utilizing the increased viscosity to sweep oil residuals from reservoirs, and thus, various types of polymers are available in the market. The salinity of the oil reservoirs is a key question in EOR processes since the chemical composition and concentration of salts in the underground water highly affect the viscoelastic properties of the EOR polymers. Here, four types of commercially available polymers containing AAM, AAC, and AMPS and hydrophilic monomers were studied, considering rheology, size, and charge features in aqueous solutions. The salinity-dependent coherent–incoherent (gel–sol) structural transitions were characterized by the transition salt concentration (TSC) values, which were sensitive to the valence of the counterions in the systems. The TSC data were also dependent on the rheology setup (rotational or oscillation), indicating the importance of the flow conditions in the oil reservoirs. The obtained data revealed that kosmotrope ions such as Ca^{2+} are efficient in stabilizing the sol, i.e., macromolecular solution, state in contrast to chaotrope ions like Na^+ , whose presence led to higher TSC values. Other polymer–counterion interactions such as ion binding and charge screening also play crucial roles in the structure formation, size, and charge features of the polymers. The reported data are important to choose polymer solutions for EOR applications in reservoirs of different salinities.



1. INTRODUCTION

The world's economy still strongly relies on existing oil resources, and efficient recovery is the subject of academic and engineering research activities, as indicated by recent reviews.^{1–3} In many reservoirs, a significant amount of crude oil remains after water flooding, which can be exploited during enhanced oil recovery (EOR) including processes using various chemicals such as polymers,^{4,5} surfactants,^{2,6} or other substances.^{7,8} Besides chemical-based EOR, various physical methods such as gas injection³ or heat treatment⁹ have also proven to be successful in the tertiary recovery of oil residuals.

Regarding polymer flooding, natural¹⁰ and synthetic¹¹ macromolecules are both potential candidates in EOR, alone or together with additives.^{12,13} For instance, during surfactant–polymer flooding, the amphiphilic molecules gradually decrease the surface tension, and the improved displacing effect and mobility ratio induced by the polymer lead to an increased sweep efficiency.^{14,15} The main requirements for EOR polymers include an optimal molecular weight range, filterability and stability, parameters that are responsible for the solution structure, and subsequent rheological features, as well as durability under the experimental conditions present in the reservoir. As frequently used EOR polymers, partially hydrolyzed polyacrylamides showed good efficiency in tertiary recovery processes, while such an efficiency remarkably

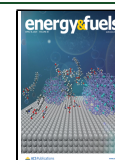
decreased at extreme environmental conditions, e.g., at high salinity or elevated temperature.¹⁶ These facts prompted the idea to use novel polymers showing considerable resistance in their viscosity and transport processes in porous media against changes in salinity and temperature.¹⁷ It is evident that the viscoelastic properties of the polymers highly influence their applicability in EOR technologies, and these features must be tuned according to the experimental conditions in the reservoirs. In general, polymer chains assemble in coherent structures (gel) at a high concentration and low salinity due to the intermolecular interactions of hydrophobic, electrostatic, or hydrogen bonding origin.^{16,18} Such an interconnected gel-like structure gives rise to improved viscosity and sweep efficiency. Nevertheless, elevated salt levels and the presence of multivalent ions often induce the collapse of coherency, and thus, macromolecular solutions (sol) containing individual, separated polymer chains form.¹⁷

Received: January 25, 2024

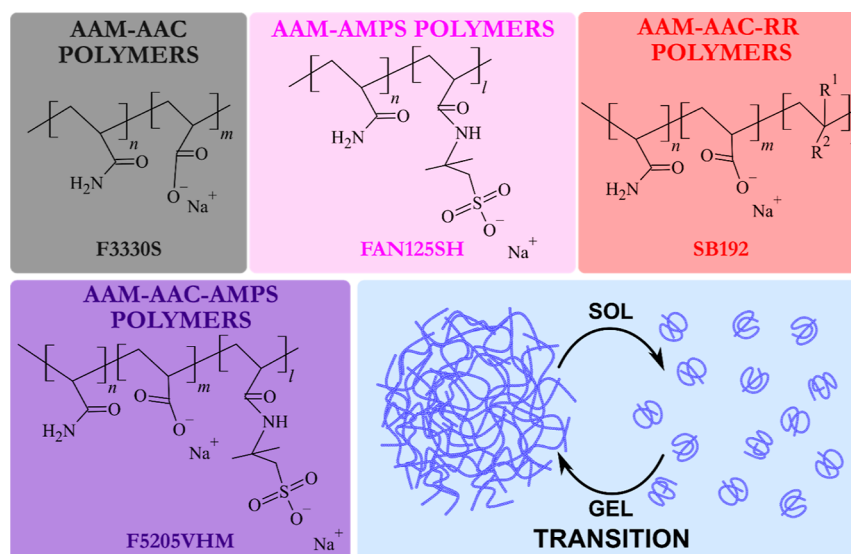
Revised: March 26, 2024

Accepted: March 28, 2024

Published: April 8, 2024



Scheme 1. Chemical Structures of the Monomeric Units in the AAM-AAC, AAM-AMPS, AAM-AAC-RR, and AAM-AAC-AMPS EOR Polymers Investigated in the Present Work^a



^aAAM, AAC, and AMPS indicate acrylamide, acrylic acid, and 2-acrylamido-2-methylpropane sulfonic acid monomers, respectively. RR means hydrophobic segments, while R¹ and R² mark different kinds of hydrophobic blocks. The principle of the sol–gel transition process is also indicated.

Such a sol–gel transition depends not only on the salinity and polymer concentration but also on other factors like temperature, chemical composition, and porosity of the oil reservoir, while it can be tuned by additives including surfactants,^{15,19} solid particles,^{20–23} or other surface active compounds.^{8,12} It is obvious from these facts that a direct comparison of the efficiency of EOR polymers can be given only under the same reservoir conditions due to the sensitivity of the sol–gel transition process to environmental factors.^{2,16}

The role of the ionic environment present in the reservoirs is of particular importance since ion-specific effects are responsible for the structural and physicochemical properties of polymer or polymer–surfactant solutions.²⁴ The effect of the chemical composition of the electrolyte on the structure of polymers (or their charged version called polyelectrolytes) has already been reported in the past and was explained with the Hofmeister series of ions.^{25–27} Accordingly, the presence of kosmotropes (or water-structure-forming ions) stabilizes the conformation of well-hydrated polymeric chains, while chaotropes (or water-structure-breaking ions) disturb the hydrogen bonding pattern in polymer solutions and, hence, lead to the unfolding of the macromolecules.²⁸ Despite its clear importance, such an ion-specific effect induced by dissolved salt constituents has rarely been studied and compared for EOR polymers.

Therefore, the present work aims at the comprehensive investigation of the structural, rheological, and charging features of EOR polymers including poly(acrylamide-*co*-acrylic acid) (AAM-AAC), poly(acrylamide-*co*-acrylamido-methylpropanesulfonic acid) (AAM-AMPS), their combination (AAM-AAC-AMPS, see Scheme 1), and an associative polymer (AAM-AAC-RR) in salt solutions. The salinity level, chemical composition, and valence of the electrolytes were varied in a wide range to explore possible effects on the solution and viscoelastic properties. Rotational and oscillatory rheology as well as light scattering techniques were applied to obtain insights into the sol–gel transition phenomenon of the

polymers. The results are useful in the selection of EOR polymers for oil recovery processes in reservoirs of known salinity, i.e., where the salt concentrations and compositions were determined prior to chemical EOR process design.

2. EXPERIMENTAL SECTION

2.1. Materials. The polymers with polyacrylamide backbones [Flopaam 3330 S (F3330S), reported molar mass of 8000 kDa; Flopaam AN 125 SH (FAN125SH), 8000 kDa; Superpusher B 192 (SB192), 10,000 MDa; and Flopaam 5205 VHM (F5205VHM), 13,000 Da] were received from SNF Group through MOL Plc. Chemicals such as NaCl, KCl, CaCl₂, and MgCl₂ were purchased from VWR and used without purification.

2.2. Sample Preparation. Ultrapure water produced with an ADRONA B30 device was used to prepare the solutions. The dust contamination was eliminated from the electrolyte solutions by filtration using a 0.1 μm PVDF filter (Millex). In general, a calculated amount of polymer powder was added to water or to the desired salt solutions to reach a 5 g/L polymer concentration in the stock samples, which were stirred overnight using a magnetic stirrer. Dilution series were prepared from the above stocks by taking calculated amounts from the most concentrated saline polymer solution and diluting them with a solution containing ultrapure water and the polymer in 1 g/L concentration. The salt concentration in the final samples was in the range of 0.03–270 g/L, and a change in salinity did not affect the solubility of the polymers. The sample preparation procedure and all measurements were performed at 25 °C.

2.3. Rheology Investigation. Oscillation and rotational rheology experiments were carried out with an Anton Paar MCR 302 device by applying a thermostated double-gap geometry. The experimental details and protocols are described elsewhere.¹⁸

2.4. Electrophoresis. To assess the charge features of the polymers in electrolyte solutions, the phase analysis light scattering method was used (Litesizer 500, Anton Paar) using the Univette accessory. The zeta potentials (ζ) were calculated from the electrophoretic mobility (*u*) data using the Smoluchowski model as²⁹

$$\zeta = u\eta/\epsilon_r\epsilon_0 \quad (1)$$

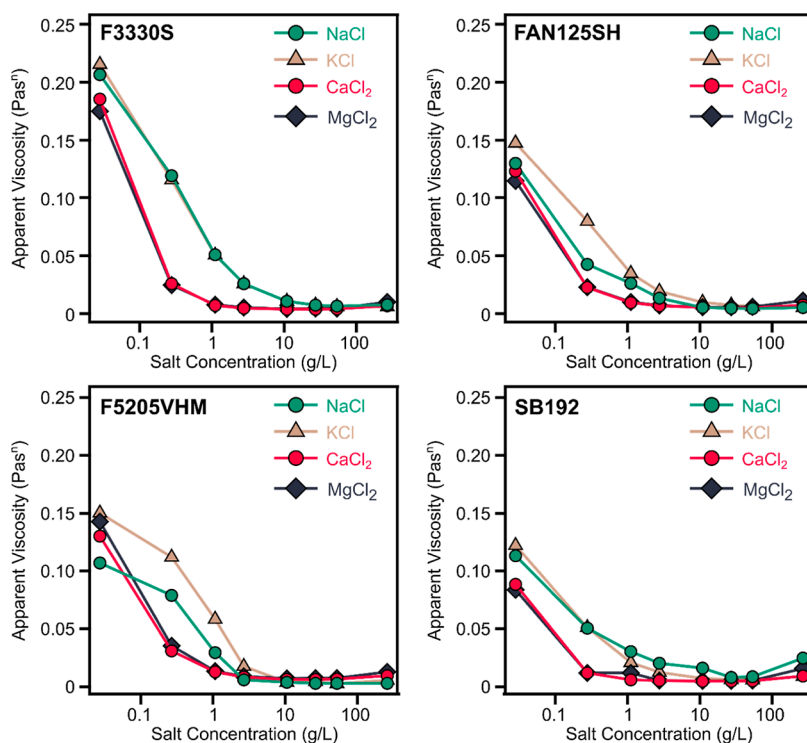


Figure 1. Apparent viscosity data (eq 4) for the F3330S, FAN125SH, F5205VHM, and SB192 polymers in NaCl, KCl, CaCl₂, and MgCl₂ solutions of different concentrations. The solid lines guide the eyes.

where $\epsilon_r \epsilon_0$ is the permittivity and η is the dynamic viscosity of the medium. The reported zeta potential data represent the average of five independent measurements. Note that zeta potential measurements were performed only up to 27 g/L salt concentrations to avoid polarization of the electrodes and Joule heating.

2.5. Dynamic Light Scattering. The polymer size (hydrodynamic radius, R_h) was determined using the recently developed modulated 3D cross-correlation dynamic light scattering (DLS) technique³⁰ to avoid multiple scattering events in concentrated samples. The measurements were carried out with an LS spectrometer (LS Instruments). The correlation function was collected at a 90° scattering angle and fitted with the COREEN algorithm. The diffusion coefficient (D) was calculated from the decay rate of the correlation (Γ) as follows³¹

$$D = \Gamma/q^2 \quad (2)$$

where q refers to the numerical value of the scattering vector. D was converted to R_h with the Stokes–Einstein relation as³²

$$R_h = k_B T / 6\pi\eta D \quad (3)$$

where k_B is the Boltzmann constant and T is the temperature. The reported values are the means of five DLS measurements.

3. RESULTS AND DISCUSSION

3.1. General Remarks on the EOR Polymers. Four types of EOR polymers were studied in the present work. First, the F3330S copolymer contains AAM and AAC monomers with 25–30 mol % ionicity, which refers to the deprotonated carboxylic groups of AAC monomers. Second, FAN125SH consists of uncharged and charged monomers, AAM and AMPS, respectively. The deprotonation of the latter one leads to a 25 mol % ionic content. Third, F5205VHM is of complex structure as all three (AAM, AAC, and AMPS) above-mentioned monomers are present in the chain, leading to an ionicity of 25 mol % due to the ionization of carboxylic and sulfonic groups at appropriate pH values. Fourth, among the

AAM units, SB192 contains other uncharged monomers of hydrophobic alkyl chains, while the 10–15 mol % line charge originates from the deprotonation of carboxylic groups in AAC. In the latter polymer, the hydrophobic segments were reported to play a critical role in the salt resistance of the rheological features.³³ Note that all of these macromolecules can be considered polyelectrolytes owing to their significant line charge density.

3.2. Effect of Salts on the Polymer Flow. Rotational rheology was used to explore the flow properties of the four polymers (F3330S, FAN125SH, SB192, and F5205VHM). First, the flow curves (Figure S1 in the Supporting Information) were recorded to measure shear stress (τ) data. The samples were also measured from 1000 to 1 s⁻¹, but hysteresis was not observed. In general, nonlinear shapes of the flow curves were observed for each type of polymer at low salinity, which indicates pseudoplastic flow properties and, subsequently, the formation of a coherent (gel) structure.³⁴ Besides, the linear shear rate versus shear stress relation at higher salt levels indicates the existence of Newtonian behavior and the presence of macromolecular solutions (sol) without significant interaction between the polymer chains.¹⁸ This generic tendency, i.e., gel–sol transition by increasing the salinity, was independent of the type of polymers and salts and has been reported earlier for charged polymers used in EOR processes.^{10,16,17} The mechanism underlying this phenomenon involves charge screening,³⁵ ion pairing,³⁶ and condensation³⁷ involving the dissolved salt constituents, especially the counterions, which are the cations in this case.

To compare the gel–sol transition of the polymers of different backbones and functional groups in a more quantitative manner, the flow curves were analyzed with the Herschel–Bulky equation as³⁸

$$\tau = \tau_0 + k\dot{\gamma}^n \quad (4)$$

where τ_0 is the yield stress and equal to the minimum shear of the irreversible plastic deformation, n refers to the flow number, and k is the apparent viscosity, which is related to the resistance of the polymer solution against the flow. These data were found to be sensitive to the gel–sol transitions of polymers.^{18,39} The ones determined in this study are shown in Figure 1 (apparent viscosity) and Figure S2 (yield stress and flow number).

Note that the increase in the flow number indicates the gel–sol transition, while this process leads to a decrease in the yield stress and apparent viscosity data. It was found that the change in the latter parameter is more appropriate to determine the transition salt concentration (TSC), which separates the salt regimes in which coherent (gel) or incoherent (sol) structures form. The data in these regions were fitted with linear regressions, and the cross points yielded the TSC values, as represented by an example in Figure S3. The TSC data determined in all polymer–salt solutions on the basis of the salt concentration dependence of the magnitude of the apparent viscosities are shown in Figure 2. Note that the TSC data determined from the other two Herschel–Bulkley parameters (Figure S2) also followed the same tendency.

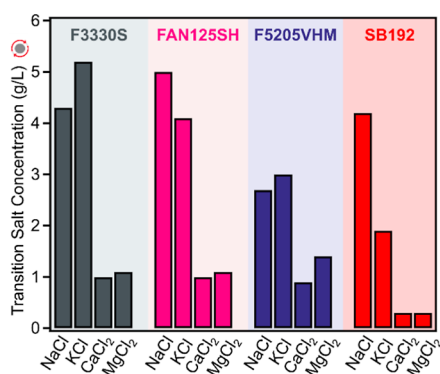
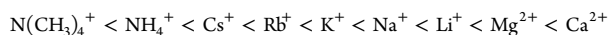


Figure 2. TSC data were determined in rotational rheology measurements using the apparent viscosity data for all polymer–salt systems studied.

The results in Figure 2 indicate that the TSC values were always higher in monovalent salts than those in the presence of multivalent cations. Such a difference was more pronounced for F3330S and FAN125SH compared to 5205VHM and SB192, which have a more complex structure. The Hofmeister series of cations for negatively charged polymeric compounds predicts the following order in terms of stabilization of individual chains^{27,40,41}



The above order defines ions on the right side as kosmotropes, which stabilize the conformation of well-hydrated polymeric chains, while the left-hand side ones are the chaotropes with water-structure-breaking ability, i.e., they tend to disturb the hydrogen network and, subsequently, destabilize polymers or polyelectrolytes in solution. Accordingly, in the presence of Ca^{2+} and Mg^{2+} ions, the polymers form a solution of individual chains (sol) already at lower salt concentrations, while Na^+ and K^+ cations did not affect the coherent (gel) structure at such a low salinity. The data presented are in line with this explanation since the TSC values

are lower for the divalent counterions and higher for the monovalent ones. Moreover, the TSC data for Mg^{2+} ions are always slightly higher than those for Ca^{2+} , in line with the Hofmeister series. Nevertheless, no unambiguous trend was observed with the monovalent cations. Obviously, other interactions than ion-specific effects may also act during destabilization of the coherent structure by increasing the salinity, and they involve electrostatic charge screening,^{33,42,43} for instance.

To further explore the flow features in the polymer–salt solutions, oscillation rheology experiments were performed. The viscoelastic properties and, hence, the gel–sol transitions were characterized by the alteration of the shear storage modulus (G') and the shear loss modulus (G''), resulting in a loss factor ($\tan \delta$)⁴⁴

$$\tan \delta = G''/G' \quad (5)$$

The G' value indicates the energy storage by the elastic structure, while G'' indicates the energy dissipated in the sample. Accordingly, if G' and G'' are equal, the viscoelastic property appears (gel), while they are different by orders of magnitude in the case of macromolecular solutions (sol). Therefore, their ratio, the loss factor, was found to be appropriate to follow gel–sol transitions in the polymer solutions studied (Figure 3). The value of the loss factor is infinite in the case of viscous liquids and zero for elastic samples. A substance is in the process of changing from a liquid to a solid form if its loss factor is 1. The term “gel point” refers to this transition point.

In all samples, loss factor values were close to unity at low salt concentrations, indicating the coherent structures, and they suddenly increased at higher salinity due to the formation of the macromolecular solutions. Accordingly, the salt-induced gel–sol transition could be clearly detected by these data, from which the TSC values were also determined by fitting the points with a mathematical function (see Figure S4 in the Supporting Information). The TSC data determined from the loss factor versus salt concentration data are shown in Figure S5. There are two observations that deserve discussion. First, the TSC values are at least a factor of 2 lower than the ones determined in rotational rheology measurements. This could be due to the sensitivity of the different techniques applied. This issue may be addressed in a future study by combining experimental and theoretical approaches. Second, the differences between the TSC measured for mono- and multivalent ions are striking for FAN125SH and F5205VHM, while they are moderate for SB192 and not unambiguous for F3330S. These results indicate that TSC determination can be performed by these techniques; however, the flow conditions in the reservoir should also be considered prior to choosing the method.

3.3. Hydrodynamic Size Assessment. The structural aspects of the above gel–sol transition were further investigated by measuring the hydrodynamic radius of the polymers over a wide range of salt concentrations (Figure S6). At salt levels below the TSC, where a coherent state of the polymers is expected on the basis of the rheology results, the DLS measurements were not reliable and reproducible. Nevertheless, at salinity above the TSC, this problem was not observed, and the hydrodynamic radius values were determined with low experimental errors. To address this issue, the intensity correlation functions were investigated, and it was found that they do not follow the exponential decay at low salt

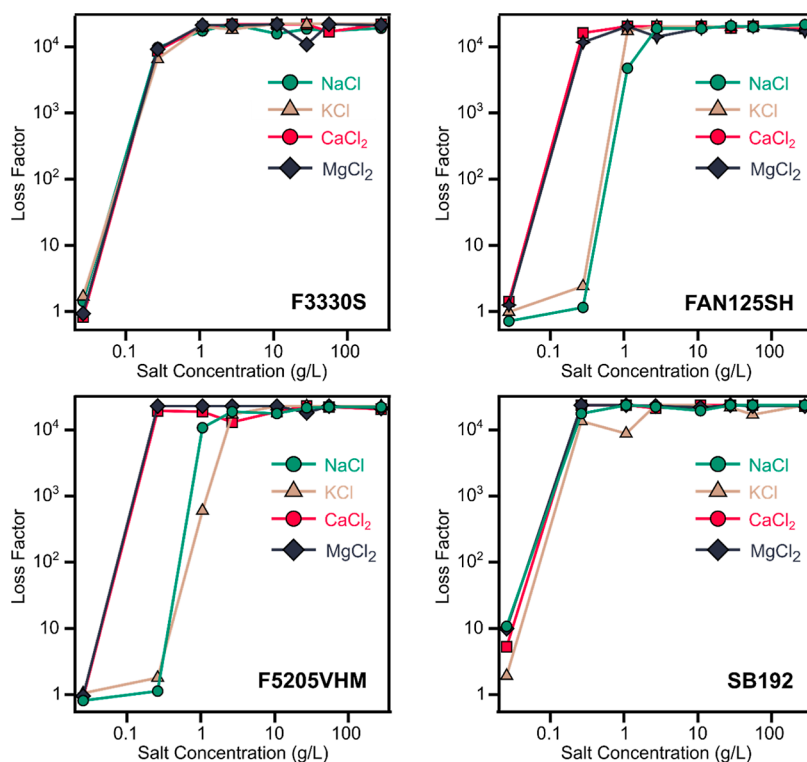


Figure 3. Loss factor data were determined from the loss and storage moduli (eq 5) for the F3330S, FAN125SH, SB192, and F5205VHM polymers as a function of the salt (NaCl, KCl, CaCl₂, and MgCl₂) concentration. Lines are eye guides.

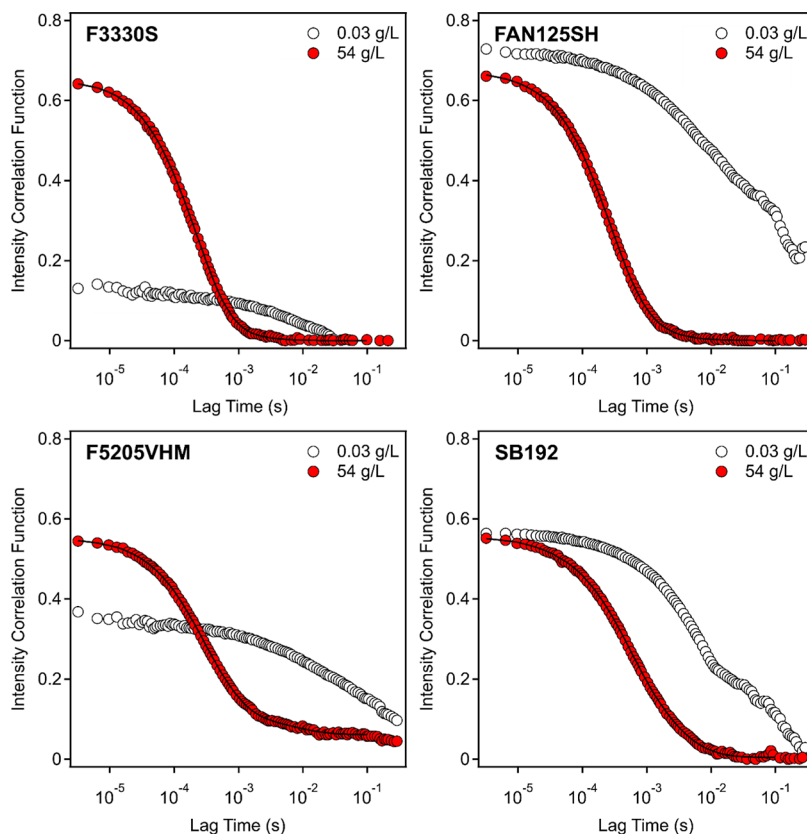


Figure 4. DLS intensity correlation function versus the lag time for the polymer (F3330S, FAN125SH, SB192, and F5205VHM) solutions below (0.03 g/L, marked with empty circles) and above (54 g/L, marked with red circles) the TSC in NaCl solutions. The solid lines fit the CORENN algorithm, and the symbols are the experimentally measured values.

concentrations, but the tendencies rather confirm the presence of a coherent structure^{45,46} with no individual macromolecular chains. Besides, an exponential decay was observed at higher salt levels, above the TSC (Figure 4), indicating the Brownian motion³¹ of the individual polymer chains without significant interactions between them.

These facts clearly confirm the gel–sol transition again by increasing the salinity of the solutions. The hydrodynamic radii determined at 54 g/L, above the TSC in all systems, are compared in Figure 5.

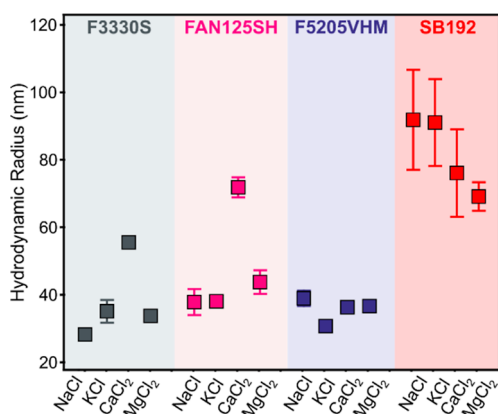


Figure 5. Hydrodynamic radius data for the F3330S, FAN125SH, SB192, and F5205VHM polymers determined in salt (NaCl, KCl, CaCl₂, and MgCl₂) solutions of 54 g/L concentration.

The radii were always below 100 nm, as expected from individual polymeric chains. For F3330S and FAN125SH, the radii were slightly higher in the presence of Ca²⁺ ions, the phenomenon of which was absent for F5205VHM and SB192 of more complex structures and higher molecular mass. Apart from this observation, the type of other ions did not affect the size of the polymers significantly, and the hydrodynamic radii were very close to each other for the same polymer and different salts. These findings indicate that ion-specific effects on the size of individual macromolecules are not remarkable in the systems studied. The increase in the values in the F3330S or FAN125SH-Ca²⁺ systems can be explained by the kosmotropic character of the divalent ion (see Hofmeister series of cations above), which favors hydrogen bonding, i.e., hydration of the polymer, giving rise to higher hydrodynamic radius values. The absence of this effect for the F5205VHM and SB192 polymers can be likely explained by their high molecular mass, at which the size is determined by other factors such as intramolecular interactions between the polymer segments.

3.4. Salinity-Dependent Charge Features. The zeta potentials were measured at similar conditions as the hydrodynamic size in the DLS study; nevertheless, the highest salt concentration was always 27 g/L due to the limitations of the instrument used. The full set of data is shown in Figure S7. In all polymer-salt systems, the zeta potentials increased with an increase in the salt concentration. The trends and the data were very similar for the mono (KCl and NaCl) as well as the divalent (CaCl₂ and MgCl₂) salts in the individual systems, indicating that the valence of the counterions determines the charge properties of the polymers. Such an effect of counterion valence on the zeta potentials is striking, especially in the intermediate salt concentration regimes, in which about 15 mV

differences were measured between the data determined for mono- or divalent salts. Such a difference is due to the joint effect of the charge correlation between the counterions and the polymer charges,³⁶ in addition to the higher ionic strength in the multivalent salt solutions at the same total salt concentrations. The latter condition gives rise to more pronounced salt screening^{35,43} and thus lower magnitudes of the zeta potentials, whose values measured below (0.03 g/L) and above (27 g/L) the TSC are presented in Figure 6.

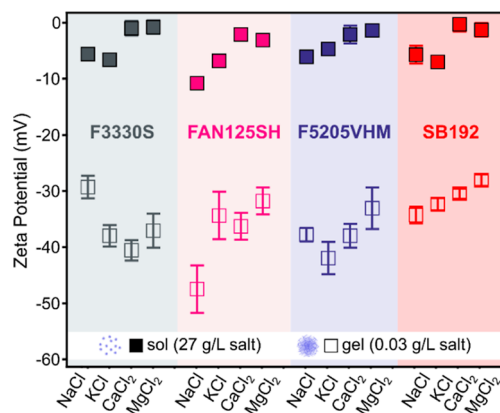


Figure 6. Zeta potential data for the F3330S, FAN125SH, SB192, and F5205VHM polymers determined in salt (NaCl, KCl, CaCl₂, and MgCl₂) solutions of 0.03 and 27 g/L concentrations.

The electrophoretic measurements performed at a low salt level, i.e., at conditions where rheology results indicated the formation of the coherent structure, yielded highly negative zeta potentials. Since the gel-like state gave rise to a relatively high standard deviation of the data, no unambiguous tendencies could be observed by changing the composition of the salts. However, at a 27 g/L concentration, the zeta potentials were always closer to zero for the multivalent ions, as explained above with the polymer–ion interactions. The origin of such a trend can also be discussed in terms of the Hofmeister effect since the more kosmotropic divalent ions possess higher affinity to the polymer chains, and hence, the overall charge of the macromolecules becomes smaller in magnitude. In other words, divalent ions are more effective in charge screening due to ion-specific effects and also more efficiently break the coherent structure by stabilizing the macromolecular solution in the incoherent state.

4. CONCLUSIONS

In conclusion, the rheology, size, and charge properties of four EOR polymer solutions were systematically investigated in salt solutions of different ionic valences and concentrations. In general, the polymers form coherent structures (gel) at low salinity, while such a structure collapses and macromolecular solution (sol) forms at the TSC, which is a characteristic salt concentration for such a gel–sol transition. The main parameter that influences the TSC values is the valence of the counterions, and multivalent ions were found to be more effective to stabilize polymer solutions due to their kosmotropic nature, as predicted by the Hofmeister series of cations developed for negatively charged macromolecules. Applying different methodologies in rheology experiments resulted in a systematic deviation of the TSC values. The hydrodynamic size of the polymers was sensitive to the ionic

environment, especially in the case of F3330S and FAN125SH, leading to the largest size obtained in the presence of structure-making Ca^{2+} ions. The hydrodynamic radius of more complex polymers such as F5205VHM and SB192 was less sensitive to the type of ions present. Zeta potential data depended mostly on the valence of counterions, and multivalent ions reduced the charge of the polymers more effectively. The main conclusion of the present study is that the structure, size, and charge of the polymers depend on specific polymer-counterion interactions including binding, screening, and condensation by the dissolved salt constituent cations. Besides, such ion-specific effects and the type of counterions play a very important role in determining the solution features, even a more pronounced one than the chemical composition of the polymers. These findings are of importance in the selection of the appropriate properties of macromolecules to be applied in polymer flooding processes in reservoirs with known total salinity, ionic composition, and flow conditions.

■ ASSOCIATED CONTENT

SI Supporting Information

The Supporting Information is available free of charge at <https://pubs.acs.org/doi/10.1021/acs.energyfuels.4c00423>.

Data of rotational and oscillation rheology measurements, hydrodynamic radius, and zeta potential values (PDF)

■ AUTHOR INFORMATION

Corresponding Author

Istvan Szilagyi – MTA-SZTE Momentum Biocolloids Research Group, Department of Physical Chemistry and Materials Science, University of Szeged, H-6720 Szeged, Hungary; orcid.org/0000-0001-7289-0979; Email: szistvan@chem.u-szeged.hu

Authors

Zsófia Vargáné Árok – MTA-SZTE Momentum Biocolloids Research Group, Department of Physical Chemistry and Materials Science, University of Szeged, H-6720 Szeged, Hungary

Szilárd Sáringer – MTA-SZTE Momentum Biocolloids Research Group, Department of Physical Chemistry and Materials Science, University of Szeged, H-6720 Szeged, Hungary

Gréta Papp – MTA-SZTE Momentum Biocolloids Research Group, Department of Physical Chemistry and Materials Science, University of Szeged, H-6720 Szeged, Hungary

Ádám Juhász – MTA-SZTE Momentum Biocolloids Research Group, Department of Physical Chemistry and Materials Science, University of Szeged, H-6720 Szeged, Hungary; MTA-SZTE Momentum Noble Metal Nanostructures Research Group, Department of Physical Chemistry and Materials Science, University of Szeged, H-6720 Szeged, Hungary

Sándor Puskás – Oilfield Chemicals and Technologies, MOL Plc, H-6701 Szeged, Hungary

Complete contact information is available at <https://pubs.acs.org/doi/10.1021/acs.energyfuels.4c00423>

Notes

The authors declare no competing financial interest.

■ ACKNOWLEDGMENTS

The authors thank the National Research, Development and Innovation Office (project GINOP-2.3.4-15-2020-00006 and SNN142258) and the University of Szeged Open Access Fund (6908) for supporting the research as well as the SNF Group and the MOL Plc for the polymer samples.

■ REFERENCES

- (1) Chowdhury, S.; Shrivastava, S.; Kakati, A.; Sangwai, J. S. Comprehensive review on the role of surfactants in the chemical enhanced oil recovery process. *Ind. Eng. Chem. Res.* **2022**, *61*, 21–64.
- (2) Chen, W. D.; Geng, X. F.; Liu, W. D.; Ding, B.; Xiong, C. M.; Sun, J. F.; Wang, C.; Jiang, K. A comprehensive review on screening, application, and perspectives of surfactant-based chemical-enhanced oil recovery methods in unconventional oil reservoirs. *Energy Fuels* **2023**, *37*, 4729–4750.
- (3) Li, X. F.; Peng, B.; Liu, Q.; Liu, J. W.; Shang, L. W. Micro and nanobubbles technologies as a new horizon for CO₂-EOR and CO₂ geological storage techniques: A review. *Fuel* **2023**, *341*, 127661.
- (4) Liu, J. C.; Almakimi, A.; Wei, M. Z.; Bai, B. J.; Ali Hussein, I. A comprehensive review of experimental evaluation methods and results of polymer micro/nanogels for enhanced oil recovery and reduced water production. *Fuel* **2022**, *324*, 124664.
- (5) Yuan, S. D.; Liu, S. S.; Zhang, H.; Yuan, S. L. Understanding the role of host-guest interactions in enhancing oil recovery through β -cyclodextrin and adamantane modified copolymer. *J. Mol. Liq.* **2023**, *369*, 120841.
- (6) Kamal, M. S. A Review of gemini surfactants: Potential application in enhanced oil recovery. *J. Surfactants Deterg.* **2016**, *19*, 223–236.
- (7) Tackie-Otoo, B. N.; Ayoub Mohammed, M. A.; Yekeen, N.; Negash, B. M. Alternative chemical agents for alkalis, surfactants and polymers for enhanced oil recovery: Research trend and prospects. *J. Pet. Sci. Eng.* **2020**, *187*, 106828.
- (8) Somoza, A.; Tafur, N.; Arce, A.; Soto, A. Design and performance analysis of a formulation based on SDBS and ionic liquid for EOR in carbonate reservoirs. *J. Pet. Sci. Eng.* **2022**, *209*, 109856.
- (9) Thomas, S. Enhanced oil recovery - An overview. *Oil Gas Sci. Technol.* **2008**, *63*, 9–19.
- (10) Ferreira, V. H. S.; Moreno, R. Experimental evaluation of low concentration scleroglucan biopolymer solution for enhanced oil recovery in carbonate. *Oil Gas Sci. Technol.* **2020**, *75*, 61.
- (11) Data, M. J.; Milanesio, J. M.; Martini, R.; Strumia, M. Synthesis techniques for polymers applied to enhanced oil recovery. *MOJ Polym. Sci.* **2018**, *2*, 17–20.
- (12) Sakthivel, S.; Gardas, R. L.; Sangwai, J. S. Effect of alkyl ammonium ionic liquids on the interfacial tension of the crude oil-water system and their use for the enhanced oil recovery using ionic liquid-polymer flooding. *Energy Fuels* **2016**, *30*, 2514–2523.
- (13) Marx, N.; Fernandez, L.; Barcelo, F.; Spikes, H. Shear thinning and hydrodynamic friction of viscosity modifier-containing oils. Part I: Shear thinning behaviour. *Tribol. Lett.* **2018**, *66*, 92.
- (14) Olajire, A. A. Review of ASP EOR (alkaline surfactant polymer enhanced oil recovery) technology in the petroleum industry: Prospects and challenges. *Energy* **2014**, *77*, 963–982.
- (15) Nafisifar, A.; Khaksar Manshad, A.; Reza Shadizadeh, S. Synergistic study of xanthan-gum based nano-composite on PELS anionic surfactant performance, and mechanism in porous media: Microfluidic & carbonate system. *Fuel* **2023**, *348*, 128510.
- (16) Alzaabi, M. A.; Leon, J. M.; Skauge, A.; Masalmeh, S. Analysis and simulation of polymer injectivity test in a high temperature high salinity carbonate reservoir. *Polymers* **2021**, *13*, 1765.
- (17) Liang, K.; Han, P. H.; Chen, Q. S.; Su, X.; Feng, Y. J. Comparative study on enhancing oil recovery under high temperature and high salinity: Polysaccharides versus synthetic polymer. *ACS Omega* **2019**, *4*, 10620–10628.

- (18) Vargáné Árok, Z.; Sáringer, S.; Takács, D.; Bretz, C.; Juhász, Á.; Szilágyi, I. Effect of salinity on solution properties of a partially hydrolyzed polyacrylamide. *J. Mol. Liq.* **2023**, *384*, 122192.
- (19) Molinier, V.; Klimenko, A.; Passade-Boupat, N.; Bourrel, M. Insights into the intimate link between the surfactant/oil/water phase behavior and the successful design of (alkali)-surfactant-polymer floods. *Energy Fuels* **2021**, *35*, 20046–20059.
- (20) Wang, W. C.; Peng, Y.; Chen, Z. X.; Liu, H. Q.; Fan, J.; Liu, Y. S. Synergistic effects of weak alkaline-surfactant-polymer and SiO₂ nanoparticles flooding on enhanced heavy oil recovery. *Energy Fuels* **2022**, *36*, 7402–7413.
- (21) Alnarabiji, M. S.; Husein, M. M. Application of bare nanoparticle-based nanofluids in enhanced oil recovery. *Fuel* **2020**, *267*, 117262.
- (22) Buitrago-Rincon, D. L.; Sadtler, V.; Mercado, R. A.; Rques-Carmes, T.; Marchal, P.; Muñoz-Navarro, S. F.; Sandoval, M.; Pedraza-Avella, J. A.; Lemaitre, C. Silica nanoparticles in Xanthan Gum solutions: Oil recovery efficiency in core flooding tests. *Nanomaterials* **2023**, *13*, 925.
- (23) Zapata, K.; Moncayo-Riascos, I.; Céspedes, S.; Aguirre-Giraldo, A.; Corredor, L. M.; Quintero, H.; Manrique, E.; Cortés, F. B.; Ribadeneira, R.; Franco, C. A. Effect of amine-functionalized nanoparticles (SiO₂/amine) on HPAM stability under chemical degradation environments: An experimental and molecular simulation study. *Energy Fuels* **2023**, *37*, 8224–8236.
- (24) Kang, B. B.; Tang, H. C.; Zhao, Z. D.; Song, S. S. Hofmeister series: Insights of ion specificity from amphiphilic assembly and interface property. *ACS Omega* **2020**, *5*, 6229–6239.
- (25) Robertson, H.; Willott, J. D.; Gregory, K. P.; Johnson, E. C.; Gresham, I. J.; Nelson, A. R. J.; Craig, V. S. J.; Prescott, S. W.; Chapman, R.; Webber, G. B.; Wanless, E. J. From Hofmeister to hydrotrope: Effect of anion hydrocarbon chain length on a polymer brush. *J. Colloid Interface Sci.* **2023**, *634*, 983–994.
- (26) Klacic, T.; Bohinc, K.; Kovacevic, D. Suppressing the Hofmeister anion effect by thermal annealing of thin-film multilayers made of weak polyelectrolytes. *Macromolecules* **2022**, *55*, 9571–9582.
- (27) Kunz, W.; Henle, J.; Ninham, B. W. 'Zur lehre von der wirkung der salze' (about the science of the effect of salts): Franz Hofmeister's historical papers. *Curr. Opin. Colloid Interface Sci.* **2004**, *9*, 19–37.
- (28) Bastos-Gonzalez, D.; Perez-Fuentes, L.; Drummond, C.; Faraudo, J. Ions at interfaces: the central role of hydration and hydrophobicity. *Curr. Opin. Colloid Interface Sci.* **2016**, *23*, 19–28.
- (29) Delgado, A. V.; Gonzalez-Caballero, F.; Hunter, R. J.; Koopal, L. K.; Lyklema, J. Measurement and interpretation of electrokinetic phenomena. *J. Colloid Interface Sci.* **2007**, *309*, 194–224.
- (30) Block, I. D.; Scheffold, F. Modulated 3D cross-correlation light scattering: Improving turbid sample characterization. *Rev. Sci. Instrum.* **2010**, *81*, 123107.
- (31) Hassan, P. A.; Rana, S.; Verma, G. Making sense of Brownian motion: Colloid characterization by dynamic light scattering. *Langmuir* **2015**, *31*, 3–12.
- (32) Banyai, I.; Keri, M.; Nagy, Z.; Berka, M.; Balogh, L. P. Self-diffusion of water and poly(amidoamine) dendrimers in dilute aqueous solutions. *Soft Matter* **2013**, *9*, 1645–1655.
- (33) Ahmed, S.; Elraies, K. A.; Tan, I. M.; Hashmet, M. R. Experimental investigation of associative polymer performance for CO₂ foam enhanced oil recovery. *J. Pet. Sci. Eng.* **2017**, *157*, 971–979.
- (34) Joye, D. D. Shear rate and viscosity corrections for a Casson fluid in cylindrical (Couette) geometries. *J. Colloid Interface Sci.* **2003**, *267*, 204–210.
- (35) Starchenko, V.; Muller, M.; Lebovka, N. Sizing of PDADMAC/PSS complex aggregates by polyelectrolyte and salt concentration and PSS molecular weight. *J. Phys. Chem. B* **2012**, *116*, 14961–14967.
- (36) Borkovec, M.; Koper, G. J. M.; Piguet, C. Ion binding to polyelectrolytes. *Curr. Opin. Colloid Interface Sci.* **2006**, *11*, 280–289.
- (37) Manning, G. S. Limiting Laws and Counterion Condensation in Polyelectrolyte Solutions I. Colligative Properties. *J. Chem. Phys.* **1969**, *51*, 924–933.
- (38) Magnon, E.; Cayeux, E. Precise method to estimate the Herschel-Bulkley parameters from pipe rheometer measurements. *Fluids* **2021**, *6*, 157.
- (39) William, J. K. M.; Ponmani, S.; Samuel, R.; Nagarajan, R.; Sangwai, J. S. Effect of CuO and ZnO nanofluids in xanthan gum on thermal, electrical and high pressure rheology of water-based drilling fluids. *J. Pet. Sci. Eng.* **2014**, *117*, 15–27.
- (40) Salis, A.; Ninham, B. W. Models and mechanisms of Hofmeister effects in electrolyte solutions, and colloid and protein systems revisited. *Chem. Soc. Rev.* **2014**, *43*, 7358–7377.
- (41) Okur, H. I.; Hladilkova, J.; Rembert, K. B.; Cho, Y.; Heyda, J.; Dzubiella, J.; Cremer, P. S.; Jungwirth, P. Beyond the Hofmeister series: Ion-specific effects on proteins and their biological functions. *J. Phys. Chem. B* **2017**, *121*, 1997–2014.
- (42) Owczarz, M.; Motta, A. C.; Morbidelli, M.; Arosio, P. A colloidal description of intermolecular interactions driving fibril-fibril aggregation of a model amphiphilic peptide. *Langmuir* **2015**, *31*, 7590–7600.
- (43) Cerbelaud, M.; Bennani, Y.; Peyratout, C. Heteroaggregation between particles modified by polyelectrolyte multilayers. *Colloids Surf., A* **2022**, *650*, 129572.
- (44) Aho, J.; Syrjala, S. On the measurement and modeling of viscosity of polymers at low temperatures. *Polym. Test.* **2008**, *27*, 35–40.
- (45) Usulli, M.; Cao, Y. P.; Bagnani, M.; Handschin, S.; Nystrom, G.; Mezzenga, R. Probing the structure of filamentous nonergodic gels by dynamic light scattering. *Macromolecules* **2020**, *53*, 5950–5956.
- (46) Pusey, P. N. Dynamic light-scattering by nonergodic media. *Macromol. Symp.* **1994**, *79*, 17–30.